

Gold-Catalyzed [4C+2C] Cycloadditions of Allenedienes, including an Enantioselective Version with New Phosphoramidite-Based Catalysts: Mechanistic Aspects of the Divergence between [4C+3C] and [4C+2C] Pathways

Isaac Alonso,[†] Beatriz Trillo,[†] Fernando López,^{*,§} Sergi Montserrat,[‡] Gregori Ujaque,^{*,‡} Luis Castedo,[†] Agustí Lledós,[‡] and Jose L. Mascareñas^{*,†}

Departamento de Química Orgánica, Universidade de Santiago de Compostela, 15782 Santiago de Compostela, Spain, Departament de Química, Universitat Autònoma de Barcelona, 08193 Bellaterra, Barcelona, Spain, and Instituto de Química Orgánica General (CSIC), Juan de la Cierva, 3, 28006, Madrid, Spain

Received April 10, 2009; E-mail: joseluis.mascarenas@usc.es

Abstract: Gold(I) complexes featuring electron acceptor ligands such as phosphites and phosphoramidites catalyze the [4C+2C] intramolecular cycloaddition of allenedienes. The reaction is chemo- and stereoselective, and provides *trans*-fused bicyclic cycloadducts in good yields. Moreover, using novel chiral phosphoramidite-based gold catalysts it is possible to perform the reaction with excellent enantioselectivity. Experimental and theoretical data dismiss a cationic mechanism involving intermediate **II** and suggest that the formation of the [4C+2C] cycloadducts might arise from a 1,2-alkyl migration (ring contraction) in a cycloheptenyl Au-carbene intermediate (**IV**), itself arising from a [4C+3C] concerted cycloaddition of the allenediene. Therefore, these [4C+2C] allenediene cycloadditions and the previously reported [4C+3C] counterparts most likely share such cycloaddition step, differing in the final 1,2-migration step.

1. Introduction

Cycloaddition reactions are among the most practical and efficient methods to construct cyclic products from relatively simple, acyclic starting materials.¹ Needless to comment about the enormous potential and historical relevance of the [4 + 2] Diels–Alder cycloaddition, which is among the most powerful synthetic tools for the assembly of six-membered cyclic structures.² Achieving mild and effective Diels–Alder cycloadditions requires that the two partners have complementary electronic properties. This is usually accomplished by activating the components with electron withdrawing or releasing substituents (usually an electron deficient dienophile in combination with an electron-rich diene). In some cases, however, it has been shown that the [4C+2C] cycloaddition of nonactivated, thermally unreactive substrates can be efficiently promoted at low temperatures by employing appropriate transition metal catalysts. Most of the reported examples deal with cycloadditions between alkynes and 1,3-dienes, and are usually promoted by Rh, Ni or Pd catalysts.³ Much less common are the transition metal

catalyzed cycloadditions involving allenes instead of alkynes, although certain allene-tethered 1,3-dienes have also been shown to participate in Rh-catalyzed [4C+2C] cycloadditions to give interesting 5,6- and 6,6-fused bicyclic systems.⁴ From a mechanistic point of view, these type of reactions usually proceed through a series of metallacyclic intermediates formed through oxidative cyclization and carbometalation steps. A final reductive elimination process affords the corresponding cycloadducts and regenerates the metal catalyst.⁵

- (3) For representative examples with 1,3-diene-ynes, see: (a) Wender, P. A.; Jenkins, T. E. *J. Am. Chem. Soc.* **1989**, *111*, 6432–6434. (b) Jolly, R. S.; Luedtke, G.; Sheehan, D.; Livinghouse, T. *J. Am. Chem. Soc.* **1990**, *112*, 4965–4966. (c) McKinsty, L.; Livinghouse, T. *Tetrahedron* **1994**, *50*, 6145–6154. (d) Wender, P. A.; Smith, T. E. *J. Org. Chem.* **1996**, *61*, 824–825. (e) Gilbertson, S. R.; Hoge, G. S. *Tetrahedron Lett.* **1998**, *39*, 2075–2078. (f) Kumar, K.; Jolly, R. S. *Tetrahedron Lett.* **1998**, 3047–3048. (g) Motoda, D.; Kinoshita, H.; Shinokubo, H.; Oshima, K. *Angew. Chem., Int. Ed.* **2004**, *43*, 1860–1862. For intermolecular examples with 1,3-dienes and alkynes, see: (h) Carbonaro, A.; Greco, A.; Dall'Asta, G. *J. Org. Chem.* **1968**, *33*, 3948–3950. (i) tom Dieck, H.; Diercks, R. *Angew. Chem., Int. Ed. Engl.* **1983**, *22*, 778–779. (j) Paik, S.-J.; Son, S. U.; Chung, Y. K. *Org. Lett.* **1999**, *1*, 2045–2047. (k) Hilt, G.; Hess, W.; Harms, K. *Org. Lett.* **2006**, *8*, 3287–3290. For a related cycloaddition between unactivated vinylallenes and alkynes, see: (l) Murakami, M.; Ubukata, M.; Itami, K.; Ito, Y. *Angew. Chem., Int. Ed.* **1998**, *37*, 2248–2250. For representative examples on Hetero-Diels–Alder reactions, respectively, see: (m) Trost, B. M.; Brown, R. E.; Toste, F. D. *J. Am. Chem. Soc.* **2000**, *122*, 5877–5878. (n) Koyama, I.; Kurahashi, T.; Matsubara, S. *J. Am. Chem. Soc.* **2009**, *131*, 1350–1351.
- (4) (a) Wender, P. A.; Jenkins, T. E.; Suzuki, S. *J. Am. Chem. Soc.* **1995**, *117*, 1843–1844. (b) Trost, B. M.; Fandrick, D. R.; Dinh, D. C. *J. Am. Chem. Soc.* **2005**, *127*, 14186–14187. These type of [4C+2C] cycloadditions were also observed as side-processes in Rh-catalyzed dienyl Pauson–Khand reactions, see: (c) Wender, P. A.; Croatt, M. P.; Deschamps, N. M. *Angew. Chem., Int. Ed.* **2006**, *45*, 2459–2462.

[†] Universidade de Santiago de Compostela.

[§] Instituto de Química Orgánica General.

[‡] Universitat Autònoma de Barcelona.

(1) Carruthers, W. *Cycloaddition Reactions in Organic Synthesis*; Pergamon: Oxford, 1990; pp 1–208.

(2) (a) Oppolzer, W. In *Comprehensive Organic Synthesis*, Vol. 5; Trost, B. M., Fleming, I., Paquette, L. A., Eds.; Pergamon: Oxford, 1991; pp 315–399. For reviews on applications of Diels–Alder reactions in total synthesis, see: (b) Nicolaou, K. C.; Snyder, S. A.; Montagnon, T.; Vassilikogiannakis, G. *Angew. Chem., Int. Ed.* **2002**, *41*, 1668–1698. (c) Takao, K.; Munakata, R.; Tadano, K. *Chem. Rev.* **2005**, *105*, 4779–4807.

On the other hand, the extraordinary growth of homogeneous gold catalysis in recent years have resulted in new, entirely different mechanistic scenarios for performing formal cycloaddition reactions in unactivated, thermally unreactive substrates.⁶ In particular, carbophilic gold(I) complexes have been shown to induce [4 + 2] annulations of several types of alkyne-containing substrates.⁷ Common to these transformations are the π -activation of the triple bond toward nucleophilic attack and the participation of carbenoid gold intermediates.^{8,9}

We have recently reported that PtCl₂ and *N*-heterocyclic carbene-gold(I) complexes catalyze the intramolecular [4C(4 π)+3C(2 π)] cycloadditions of allene-tethered 1,3-dienes.¹⁰ Experimental and theoretical DFT studies agree with a mechanism involving a π -activation of the allene moiety by the metal catalyst to generate a metal-allyl cation intermediate, followed by a concerted *exo*-like cycloaddition with the diene. A subsequent 1,2-shift on the resulting cycloheptenyl metal-carbene yields the final [4C+3C] adduct and regenerates the catalyst. Overall, this method provides a straightforward and atom economical entry to a variety of cycloheptene-containing polycycles from readily available acyclic allenediene precursors. Herein, we demonstrate that the same type of allenedienes, when dialkylated at the distal position of the allene, undergo a mild [4C+2C] intramolecular cycloaddition upon treatment with a Au(I) complex featuring a phosphite ligand. The reaction is chemo- and stereoselective, and provides synthetically relevant *trans*-fused bicyclic cycloadducts (**3**) in good yields.¹¹ Furthermore, we have prepared several novel chiral phosphoramidite-based Au(I) complexes and demonstrate that some of them are able to promote the reaction in a completely chemoselective

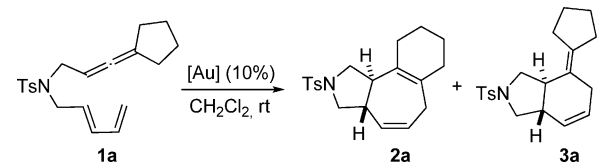
manner and with very high enantioselectivity. We also report results of experimental and theoretical mechanistic studies which do not support a reaction pathway involving stepwise cyclizations through cationic intermediates but suggest an alternative route comprising a [4C+3C] concerted cycloaddition and a subsequent ring contraction in the resulting gold-carbene intermediate. This mechanistic proposal is compatible with experimental results and accounts for the observed [4C+3C]/[4C+2C] dichotomy, however other alternatives cannot be fully discarded.

2. Results and Discussion

2.1. Au-Catalyzed [4C+2C] Cycloadditions of Allenedienes.

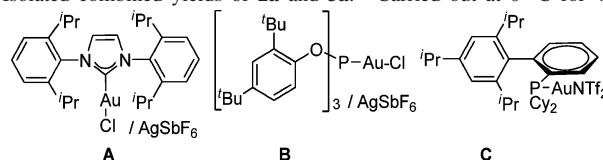
Scope and Limitations. This research aroused from the observation that the reaction of **1a** in presence of catalyst A [(IPr)AuCl/AgSbF₆] (Table 1), in addition to providing the [4C+3C] cycloadduct **2a**, led to the [4C+2C] adduct **3a** (3:1 ratio, Table 1, entry 1).^{10b,12} The [4C+2C] product must result from a Au-catalyzed process, as the reaction does not proceed under thermal conditions. The intriguing mechanistic reasons for the formation of both adducts, together with the synthetic relevance of the resulting *trans*-fused 5,6-bicycles, led us to further explore this process and seek out other Au catalysts that could improve the efficiency of the [4C+2C] cycloaddition. As can be deduced from Table 1 (entries 1–4), lowering the donor ability of the

Table 1. Au-Catalyzed [4C+2C] vs [4C+3C] Cycloaddition of **1a**^a



entry	[Au] (10 mol %)	2a:3a (ratio) ^b	yield (%) ^c
1	A	3:1	66
2	C	1.4:1	78
3	Ph ₃ PAuNTf ₂	1:1.9	71
4	Ph ₃ PAuCl/AgSbF ₆	1:2.5	78
5	(PhO) ₃ PAuCl/AgSbF ₆	1:10	55
6	B	1:7	75
7 ^d	B	1:10	72

^a [Au] (10 mol %) in CH₂Cl₂ (0.15 M) at rt for 3 h unless otherwise noted. ^b Ratio determined by ¹H NMR in the crude reaction mixtures. ^c Isolated combined yields of **2a** and **3a**. ^d Carried out at 0 °C for 4 h.

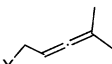
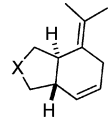
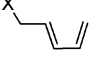
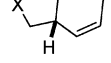


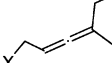
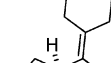
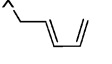
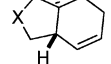
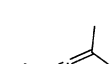
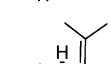
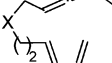
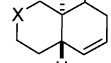

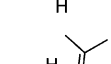
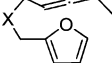
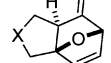

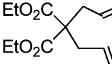
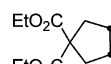


ligand at gold enhances the proportion of the [4C+2C] adduct, which becomes majoritary when PPh₃ is used as ligand (entries 3 and 4). Comparison of entries 3 and 4 suggests that the nature of the counterion also plays some role in the chemoselectivity of the cycloaddition, presumably due to differences in coordi-

- (5) (a) Wender, P. A.; Love, J. A. In *Advances in Cycloaddition*, Vol. 5.; Harmata, M., Ed.; JAI Press: Greenwich, 1999; pp 1–45. (b) Lautens, M.; Klute, W.; Tam, W. *Chem. Rev.* **1996**, *96*, 49–92. (c) Aubert, C.; Buisine, O.; Malacria, M. *Chem. Rev.* **2002**, *102*, 813–834.
- (6) For a recent review on Au-catalyzed cycloadditions, see: (a) Shen, H. C. *Tetrahedron* **2008**, *64*, 7847–7870. For recent reviews on Au-catalyzed reactions, see: (b) Li, Z.; Brouwer, C.; He, C. *Chem. Rev.* **2008**, *108*, 3239–3265. (c) Arcadi, A. *Chem. Rev.* **2008**, *108*, 3266–3325. (d) Gorin, D. J.; Sherry, B. D.; Toste, F. D. *Chem. Rev.* **2008**, *108*, 3351–3378. (e) Hashmi, A. S. K.; Rudolph, M. *Chem. Soc. Rev.* **2008**, *37*, 1766–1775. (f) Jimenez-Núñez, E.; Echavaren, A. M. *Chem. Rev.* **2008**, *108*, 3326–3350. (g) Patil, N. T.; Yamamoto, Y. *Chem. Rev.* **2008**, *108*, 3395–3442. (h) Marion, N.; Nolan, S. P. *Chem. Soc. Rev.* **2008**, *37*, 1776–1782.
- (7) For different types of Au-catalyzed [4C+2C] cycloadditions and annulations, see: (a) Nieto-Oberhuber, C.; Pérez-Galán, P.; Herrero-Gómez, E.; Lauterbach, T.; Rodríguez, C.; López, S.; Bour, C.; Rosellón, A.; Cárdenas, D. J.; Echavaren, A. M. *J. Am. Chem. Soc.* **2008**, *130*, 269–279. (b) Nieto-Oberhuber, C.; Lopez, S.; Echavaren, A. M. *J. Am. Chem. Soc.* **2005**, *127*, 6178–6179. (c) Hashmi, A. S. K.; Rudolph, M.; Weyrauch, J. P.; Wölfl, M.; Frey, W.; Bats, J. W. *Angew. Chem., Int. Ed.* **2005**, *44*, 2798–2801. (d) Fürstner, A.; Stimson, C. C. *Angew. Chem., Int. Ed.* **2007**, *46*, 8845–8849. (e) Zhang, G.; Huang, X.; Li, G.; Zhang, L. *J. Am. Chem. Soc.* **2008**, *130*, 1814–1815. (f) Lemière, G.; Gandon, V.; Cariou, K.; Hours, A.; Fukuyama, T.; Dhimane, A.-L.; Fensterbank, L.; Malacria, M. *J. Am. Chem. Soc.* **2009**, *131*, 2993–3006. (g) Barluenga, J.; Fernandez-Rodriguez, M. A.; Garcia-Garcia, P.; Aguilar, E. *J. Am. Chem. Soc.* **2008**, *130*, 2764–2765. (h) Asao, N.; Takahashi, K.; Lee, S.; Kasahara, T.; Yamamoto, Y. *J. Am. Chem. Soc.* **2002**, *124*, 12650–12651.
- (8) (a) Gorin, D. J.; Toste, F. D. *Nature* **2007**, *446*, 395–403. (b) Fürstner, A.; Davies, P. W. *Angew. Chem., Int. Ed.* **2007**, *46*, 3410–3449.
- (9) For interesting discussions about the precise nature of some of these gold carbene species and their possible consideration as gold-stabilized carbocations, see: (a) Seidel, G.; Mynott, R.; Fürstner, A. *Angew. Chem., Int. Ed.* **2009**, *48*, 2510–2513. (b) Fürstner, A.; Morency, L. *Angew. Chem., Int. Ed.* **2008**, *47*, 5030–5033. For a highlight, see: (c) Hashmi, A. S. K. *Angew. Chem., Int. Ed.* **2008**, *47*, 6754–6756.
- (10) (a) Trillo, B.; López, F.; Gullías, M.; Castedo, L.; Mascareñas, J. L. *Angew. Chem., Int. Ed.* **2008**, *47*, 951–954. (b) Trillo, B.; López, F.; Montserrat, S.; Ujaque, G.; Castedo, L.; Lledós, A.; Mascareñas, J. L. *Chem.—Eur. J.* **2009**, *15*, 3336–3339.

- (11) After initial submission of the first version of this manuscript, a paper discussing ligand-dependent divergence between [4 + 3] and [4 + 2] pathways was published by Toste et al. See: Mauleón, P.; Zeldin, R. M.; González, A. Z.; Toste, F. D. *J. Am. Chem. Soc.* **2009**, *131*, 6348–6349.
- (12) The [4C+3C] cycloaddition of **1a** can be achieved in good yields with 10 mol % of AuCl, AuCl₃ or PtCl₂. See also ref 10.

Table 2. Gold-Catalyzed [4C+2C] Cycloadditions of Allenedienes 1^a

Entry	Substrate, 1	Product	3 : 2 ^b	3 , Yield ^c
1			10 : 1	3b , 72%
2			13 : 1	3c , 79%
3			19 : 1	3c , 85% ^d
4			1 : 0	3d , 80% ^d
5			1 : 0	3e , 91%
6 ^e			1 : 0	3f , 97%
7 ^e			1 : 0	3g , 72%
8 ^e			1 : 0	3h , 84%
9 ^f			1 : 0	3i , 40%
10		-	-	3k , 0%
11			-	4k , 40% ^g

^a Conditions: (ArO)₃AuCl (10 mol %) and AgSbF₆ (10 mol %) in CH₂Cl₂ (0.15 M) at 0 °C for 1 h. ^b Ratio determined by ¹H NMR in the crude reaction mixtures. See ref 10 for data on the minor [4C+3C] adducts **2**. ^c Isolated yields. ^d Five minutes at -15 °C. ^e Forty minutes at 0 °C. ^f Sixty minutes at -40 °C. ^g Thirty minutes at 0 °C, GC yield.

nating abilities. Gratifyingly, in presence of highly electrophilic gold complexes featuring phosphite electron-acceptor ligands (entries 5 and 6), the desired [4C+2C] cycloadduct was obtained with high chemoselectivity and in a completely stereoselective manner. In particular, the use of complex **B** [(ArO)₃PAuCl/AgSbF₆],¹³ featuring a bulky phosphite ligand provided excellent results in terms of yield and selectivity. The chemoselectivity of the process could be further improved at 0 °C, without significant deterioration of the rate or yield of the process (entry 7). Thus, either cycloaddition pathway ([4 + 2] or [4 + 3]) can be suitably selected by just changing the Au catalyst, allowing to obtain synthetically relevant 5,6- and 5,7-bicyclic systems from the same allenediene substrates.

Once an optimal chemoselective protocol was established, we analyzed the scope with respect to the allenediene. Gold catalyst **B** turned to be also very effective with other allenedienes disubstituted at the allene distal position (Table 2). Thus, the [4C+2C] adducts **3b–f** were obtained in good yields, with complete *trans* selectivity and excellent chemoselectivity (Table 2, entries 1–6). Cycloadditions were typically carried out at 0 °C. However, it is worth to note that the cycloaddition of the dimethyl-substituted allenediene derivatives **1c** and **1d** can be carried out at -15 °C in just 5 min (entries 3 and 4), to give the desired cycloadducts in excellent yields. On the other hand, derivatives **1d–f** provided exclusively the [4C+2C] adducts in excellent yields (entries 4–6).

Elongation of the tethering chain was also tolerated (entry 7 and 8), providing for the assembly of *trans*-fused 6,6-bicyclic systems in a completely stereoselective manner. Interestingly, the [4 + 2] cycloaddition is particularly rapid with substrates in which the diene is embedded in a furan ring, such as **1i** (entry 8), which provides adduct **3i** in 40% yield, at -40 °C.¹⁴ It is also worth to note that the cycloadditions of allenedienes lacking the geminal-diester moiety of the tether were equally effective, as demonstrated by the cycloadditions of **1d**, **1f** and **1h**, for which the corresponding [4C+2C] adducts were obtained in 80–97% isolated yields. Confirmation of the structure and relative stereochemical assignments was unambiguously obtained by X-ray crystallographic analysis on [4C+2C] cycloadducts **3d**, **3f**, **3i**, as well as on an immediate derivative of adduct **3g**.¹⁴

The Au-catalyzed [4C+2C] cycloaddition requires that the allene is disubstituted at the distal position, as it failed in the cases of substrates **1j–k** (entries 10 and 11). Nonsubstituted allene **1j** remains unchanged after treatment with catalyst **B** at *rt* for several hours, whereas allenediene **1k**, with just one substituent at the distal position of the allene, generated a complex mixture of products, being the [2C+2C] adduct **4k** the major and only identifiable component.¹⁵ Interestingly, the rate of conversion of **1k** into **4k** is significantly lower than that of the **1b** into **3b**, demonstrating that the degree of substitution

(13) Ar = 2,4-di-*tert*-butylphenyl; For the pioneering use of this phosphite gold complex, see: López, S.; Herrero-Gómez, E.; Pérez-Galán, P.; Nieto-Oberhuber, C.; Echavarrén, A. M. *Angew* **2006**, *45*, 6029–6032. See also: (b) Gorin, D. J.; Watson, I. D. G.; Toste, F. D. *J. Am. Chem. Soc.* **2008**, *130*, 3736.

(14) See the Supporting Information for more details.

(15) For related Au-catalyzed [2C+2C] cycloadditions of allene-tethered alkenes (allenenenes), see: (a) Luzung, M. R.; Mauleón, P.; Toste, F. D. *J. Am. Chem. Soc.* **2007**, *129*, 12402–12403. See also: (b) Zhang, L. *J. Am. Chem. Soc.* **2005**, *127*, 16804–16805.

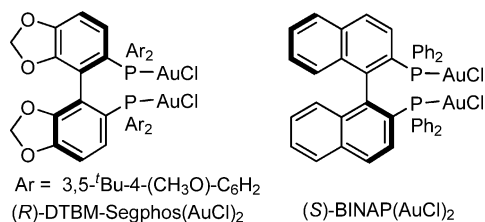


Figure 1. Bis(gold)-phosphine complexes employed in this study.

in the allene moiety has a drastic influence in its reactivity toward this gold(I) catalyst.¹⁶

2.2. Development of a Highly Enantioselective Variant with New Phosphoramidite-Based Mononuclear Gold(I) Catalysts. A New Paradigm for Asymmetric Gold Catalysis. Despite the impressive increase of reports in recent years documenting reactions catalyzed by homogeneous gold(I) complexes,⁶ so far, only a handful of these transformations have been rendered enantioselective.¹⁷ The preferred linear coordination geometry of gold(I), placing the attached ligand distant from the reactive center, has been identified as the most important obstacle to develop enantioselective processes with this metal. This linear coordination mode also precludes asymmetric strategies based on a bidentate coordination of chiral bisphosphines to the gold center, strategy particularly effective with other transition metals, such as Pd, Ru, Rh or Ir.¹⁸ Consequently, the development of enantioselective gold-catalyzed processes represents a great challenge in current homogeneous catalysis. The only example prior to 2005 was the Hayashi and Ito enantioselective aldol reactions, in which a gold(I)-ferrocenylphosphine complex behaves as a traditional Lewis acid catalyst, through carbonyl-group activation.¹⁹ More recently, bis(gold)-phosphine complexes of the form [(AuX)₂(P–P)]; (P–P) = chiral bisphosphine], such as DTBM-Segphos(AuCl)₂ (Figure 1), have emerged as versatile chiral catalysts for the development of certain enantioselective processes relying on the activation of multiple-bonds toward addition of carbon- or heteroatom-based nucleophiles.^{17,20} In particular, enantioselective cyclopropanation reactions and [2C+2C] cycloadditions of

Table 3. Asymmetric Au(I)-Catalyzed [4C+2C] Cycloadditions and Development of an Efficient Enantioselective Chiral Gold Catalyst^a

entry	[Au]	3a:2a (ratio) ^b	3a, ee (%) ^c
1	(<i>R</i>)-DTBM-Segphos(AuCl) ₂ ^d	1:1.7	8
2	(<i>S</i>)-BINAP(AuCl) ₂ ^d	1:1.2	1
3	D	3:1	—
4	(<i>S</i>)-E	6:1	2
5	(<i>S,S</i>)-F	3:1	4
6	(<i>S,S,S</i>)-G	4.5:1	20
7	(<i>R,S,S</i>)-G	3:1	4
8	(<i>S,S</i>)-H	4:1	22
9	(<i>S,S,S</i>)-I	7:1	52
10	(<i>S,R,R</i>)-I	4:1	14 ^e
11 ^{f,g}	(<i>S,S,S</i>)-I	8:1	74
12 ^{h,i}	(<i>S,S,S</i>)-I	14:1	80
13 ^{f,j}	(<i>R,R,R</i>)-J	8:1	80^e
14 ^k	(<i>R,R,R</i>)-K	8:1	84 ^e
15 ^{f,i}	(<i>R,R,R</i>)-K	16:1	91^e

^a [Au] (10 mol %) and AgSbF₆ (10 mol %) in CH₂Cl₂ (0.15 M) for 1–3 h at room temperature unless otherwise noted. Conversions into cycloadducts **3a** and **2a** > 99% (by ¹H NMR in the crude mixtures)

^b Determined by ¹H NMR in the crude mixtures. ^c Enantiomeric excess (ee) determined by HPLC (Chiralcel IA).¹⁴ ^d [Au] (5 mol %) and AgSbF₆ (10 mol %). ^e Major enantiomer is opposite to that obtained with (*S,S,S*)-I catalyst, as deduced by chiral HPLC and optical rotation. ^f Reaction carried out at –15 °C. ^g Pure **3a** isolated in 78% yield after column chromatography. ^h Reaction carried out at –30 °C. ⁱ **3a** isolated in 82% yield. ^j **3a** isolated in 73% yield. ^k **3a** isolated in 80% yield.

allenes have been proven successful with these catalytic systems.^{20e,15a} On the basis of these precedents, the performance of two of these catalysts, DTBM-Segphos(AuCl)₂ and BINAP(AuCl)₂ was initially tested for the model substrate **1a**. Unfortunately, these complexes containing moderately electron donating bisphosphine ligands were poorly chemoselective, providing mixtures of the [4C+3C] and [4C+2C] cycloadducts **2a** and **3a** (Table 3, entries 1 and 2). Moreover, the enantioselectivity of the [4C+2C] cycloadduct was very low, suggesting that the [4C+2C] process might involve a mechanism significantly different than that of the [2C+2C] cycloadditions of allenes.^{15a} On the basis of these results and considering the apparent requirement of electron acceptor ligands at gold for achieving selective [4C+2C] cycloadditions, we turned our attention to chiral gold complexes containing such type of ligands. In particular, the electronic resemblance between arylphosphites and phosphoramidites suggested the possibility of promoting these [4C+2C] cycloadditions with phosphoramidite-gold complexes of the type [L*–AuCl; L* = chiral phosphoramidite], which could eventually introduce these highly versatile and easily modulated chiral ligands into the realm of asymmetric gold catalysis.²¹ Indeed, to the best of our knowledge, these complexes have never been shown effective for any type of gold catalyzed asymmetric reaction.²²

The feasibility of performing the [4C+2C] cycloaddition with a phosphoramidite-based Au catalyst was initially tested with

- (16) Reaction of **1b** at –15 °C is almost completed in less than 10 min (> 95% conv.). At this temperature **1k** requires 90 min to reach 50% conversion.
- (17) For a review highlighting the most recent enantioselective developments, see: (a) Widenhoefer, R. A. *Chem.—Eur. J.* **2008**, *14*, 5382–5391. See also: (b) Bongers, N.; Krause, N. *Angew. Chem., Int. Ed.* **2008**, *47*, 2178–2181.
- (18) (a) Caprio, V.; Williams, J. M. J. *Catalysis in Asymmetric Synthesis*; John Wiley and Sons: Chichester, 2009. (b) Christmann, M.; Bräse, S. *Asymmetric Synthesis: The Essentials*; Wiley-VCH: Weinheim, 2007. (c) Jacobsen, E. N.; Pfaltz, A.; Yamamoto, H. *Comprehensive Asymmetric Catalysis I-III*; Springer-Verlag: Berlin, Germany, 1999. (d) Börner, A. *Phosphorus Ligands in Asymmetric Catalysis: Synthesis and Applications*; Wiley-VCH: Weinheim, 2008.
- (19) (a) Sawamura, M.; Ito, Y. In *Catalytic Asymmetric Synthesis*; Ojima, I., Ed.; VCH Publishers: New York, 1993; p 367. (b) Ito, Y.; Sawamura, M.; Hayashi, T. *J. Am. Chem. Soc.* **1986**, *108*, 6405–6406. (c) Hayashi, T.; Sawamura, M.; Ito, Y. *Tetrahedron* **1992**, *48*, 1999–2012.
- (20) For the first application of bis(gold)complexes in enantioselective catalysis, see: (a) Paz Muñoz, M.; Adrio, J.; Carretero, J. C.; Echavarren, A. M. *Organometallics* **2005**, *24*, 1293–1300. For other representative examples, see: (b) González-Arellano, C.; Corma, A.; Iglesias, M.; Sanchez, F. *Chem. Commun.* **2005**, 3451–3453. (c) Zhang, Z.; Widenhoefer, R. A. *Angew. Chem., Int. Ed.* **2007**, *46*, 283–285. (d) Tarselli, M. A.; Chianese, A. R.; Lee, S. L.; Gagné, M. R. *Angew. Chem., Int. Ed.* **2007**, *46*, 6670–6673. (e) Johansson, M. J.; Gorin, D. J.; Staben, S. T.; Toste, F. D. *J. Am. Chem. Soc.* **2005**, *127*, 18002–18003. (f) Watson, I. D. G.; Ritter, S.; Toste, F. D. *J. Am. Chem. Soc.* **2009**, *131*, 2056–2057. (g) See also ref 15a.

- (21) For representative reviews on the use of phosphoramidite ligands in other transition metal catalyzed asymmetric processes, see: **Cu**: (a) Feringa, B. L. *Acc. Chem. Res.* **2000**, *33*, 346–353. **Rh** and **Ir**: (b) Minnaard, A. J.; Feringa, B. L.; Lefort, L.; De Vries, J. G. *Acc. Chem. Res.* **2007**, *40*, 1267–1277.

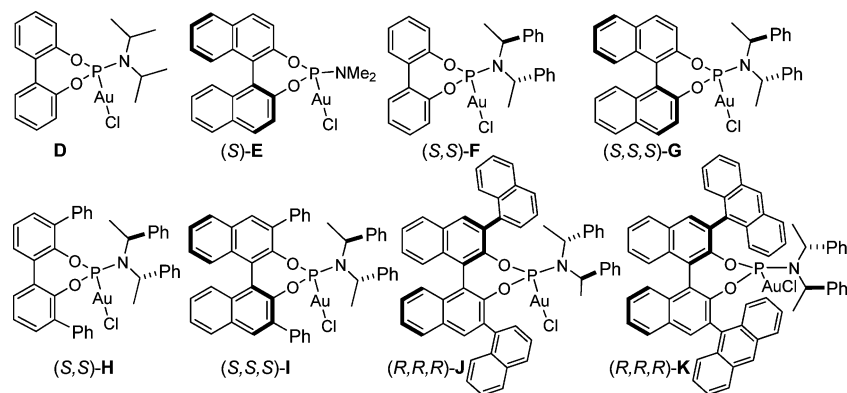


Figure 2. New chiral phosphoramidite-based gold(I) complexes.

the achiral complex **D** (Figure 2), in combination with AgSbF_6 .²³ Gratifyingly, treatment of **1a** with **D**/ AgSbF_6 (10 mol %) in CH_2Cl_2 at room temperature provided, after 1 h, full conversion to cycloadducts **3a** and **2a**, which were isolated in a good 3:1 ratio (Table 3, entry 3). Use of phosphoramidite complexes (*S,S*)-**E** or (*S,S*)-**F**, incorporating chiral groups either at the diol or amine unit, did not allow to obtain significant enantioselectivities (entries 4 and 5), but importantly, the chemoselectivity and rate of the process were not affected. Notably, a modest enantioselectivity could be obtained with complex (*S,S,S*)-**G**, which incorporates both elements of chirality, the bis(1-phenylethyl)amine moiety and the chiral binaphthol skeleton (entry 6). Analysis of results of entries 6 and 7 clearly shows that complex (*S,S,S*)-**G** corresponds to the match situation (20% ee), whereas its diastereoisomer (*R,S,S*)-**G** is a mismatched catalyst, as it provided **3a** with only 4% ee and also with lower chemoselectivity. At this point, we reasoned that introduction of bulky substituents at the 3 and 3' position of the biphenol or binaphthol units of (*S,S*)-**F** or (*S,S,S*)-**G** could positively influence the enantioselectivity of the process, since it could reduce the flexibility around the Au center, while bringing closer the chiral information to the new carbon stereocenters. Indeed, reaction with (*S,S*)-**H**, which incorporates two phenyl substituents at the 3 and 3' positions of the biphenyl unit (entry 8), provided **3a** in a somewhat higher ee than its unsubstituted analog (*S,S*)-**F** (increment of 18% ee). More importantly, gold-complex (*S,S,S*)-**I**, which incorporates the phenyl substituents at the 3 and 3' positions of the binaphthyl moiety, afforded the [4C+2C] cycloadduct **3a** with good chemoselectivity and 52% ee (32% higher than that obtained with (*S,S,S*)-**G**, entries 6 and 9).²⁴ In analogy to the results with complexes of type **G** (entries 6 and 7), the diastereoisomeric gold complex (*S,R,R*)-**I** corresponded to a mismatched situation, providing the cycloadduct **3a** with significantly lower selectivity than (*S,S,S*)-**I** (entry 10). Moreover, the major enantiomer obtained with (*S,R,R*)-**I** turned out to be the opposite to that obtained with (*S,S,S*)-**I**, indicating that the chirality of the bis(phenylethyl)amine dictates the absolute stereochemistry of the [4C+2C] cycloadduct. Gratifyingly, further optimization of the chemo- and enantioselectivity of the process could be achieved with complex (*S,S,S*)-**I**, just by lowering the temperature of the reaction (entries 11–12). Thus,

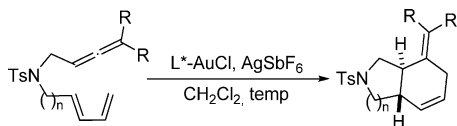
the cycloaddition of **1a** could be efficiently performed at -15 °C and even at -30 °C, providing the [4C+2C] cycloadduct **3a** in 82% yield and with 80% ee. These results clearly validate the strategy and suggested that further improvement on the enantioselectivity might be feasible by fine-tuning of substituents at 3 and 3' positions. Thus, novel bulky phosphoramidite ligands with 1-naphthyl and 9-anthracenyl substituents were synthesized and transformed into their corresponding chiral gold complexes, (*R,R,R*)-**J** and (*R,R,R*)-**K** (Figure 2). As expected, the major enantiomer obtained with these complexes turned out to be opposite to that obtained from (*S,S,S*)-**I**. Naphthyl-derived complex (*R,R,R*)-**J** provided, at -15 °C, the cycloadduct **3a** with 80% ee (entry 13), a value somewhat superior to that achieved at that temperature with the enantiomeric homologue (*S,S,S*)-**I** (entry 11). However, the 9-anthracenyl-derived analog (*R,R,R*)-**K** was much more effective, providing excellent yields of **3a** and enantioselectivities ranging from 84% at room temperature, to 91% at -15 °C (entries 14 and 15). Not less remarkable, the chemoselectivity of the process was also very high in favor of the [4C+2C] adduct **3a**.

With these results in hand, the performance of complexes (*S,S,S*)-**I** and (*R,R,R*)-**K** was next evaluated on other allenedienes. As can be deduced from Table 4, the cationic gold complex generated from (*R,R,R*)-**K** and AgSbF_6 turned out to be an excellent catalyst for these [4C+2C] cycloadditions providing, in every case, higher enantioselectivities than those obtained with its homologue (*S,S,S*)-**I**/ AgSbF_6 . Indeed, catalyst (*R,R,R*)-**K**/ AgSbF_6 afforded the corresponding cycloadducts with high to very high enantioselectivities (entries 5–8), whereas yields, chemo- and stereoselectivities are fully comparable to those previously obtained with racemic catalyst **B**. Thus, cycloadditions of allenedienes **1d**, **1f** and **1h** were completely chemoselective at -15 °C, whereas **1a** provided a high chemoselectivity. On the other hand, the enantioselectivities

(22) A chiral phosphoramidite gold catalyst has been described in ref 20a and evaluated in alkoxylation reactions of 1,6-enynes, but provided racemic products (less than 2% ee).

(23) Phosphoramidite gold complexes were prepared following procedures similar to those described in: (a) Alder, M. J.; Flower, K. R.; Pritchard, R. G. *J. Organomet. Chem.* **2001**, *629*, 153–159. (b) See also ref 20a.

(24) The introduction of substituents at the 3 and 3' positions of the binaphthol or biphenol skeletons of phosphoramidites has been proven successful in other transition metal catalyzed asymmetric processes which make use of these ligands. For representative examples, see: (a) Giacomin, F.; Meetsma, A.; Panella, L.; Lefort, L.; de Vries, A. H. M.; de Vries, J. G. *Angew. Chem., Int. Ed.* **2007**, *46*, 1497–1500. (b) Hua, Z.; Vassar, V. C.; Choi, H.; Ojima, I. *Proc. Natl. Acad. Sci. U.S.A.* **2004**, *101*, 5411–5416. Phosphoramidite ligand precursor of complex (*S,R,R*)-**I** has been proven successful in Pd-catalyzed enantioselective hydrogenolysis of arene tricarbonyl chromium(0) complexes, see: (c) Kündig, E. P.; Chaudhuri, P. D.; House, D.; Bernardinelli, G. *Angew. Chem., Int. Ed.* **2006**, *45*, 1092–1095. For beneficial effects of 3,3'-diaryl substitution on BINOL-phosphoric acids, employed as chiral Brønsted acid catalysts in several asymmetric processes, see: (d) Terada, M. *Chem. Commun.* **2008**, 4097–4112, and references therein.

Table 4. Enantioselective Au(I)-Catalyzed Allenediene [4C+2C] Cycloadditions with (*S,S,S*)-**I** and (*R,R,R*)-**K**^a


1a, R = -(CH₂)₄-; n = 1
1d, R = Me; n = 1
1f, R = -(CH₂)₅-; n = 1
1h, R = Me; n = 2

entry	1	L*-AuCl	temp. (°C)	3:2 ^b	yield ^c	3	ee, % ^{d,e}
1	1a	(<i>S,S,S</i>)- I	-30	14:1	82%	3a	80 (-)
2	1d	(<i>S,S,S</i>)- I	-15	1:0	84%	3d	76 (-)
3	1f	(<i>S,S,S</i>)- I	-15	1:0	70%	3f	86 (-)
4	1h	(<i>S,S,S</i>)- I	-15	1:0	55%	3h	52 (-)
5	1a	(<i>R,R,R</i>)- K	-15	16:1	82%	3a	91 (+)
6	1d	(<i>R,R,R</i>)- K	-15	1:0	93%	3d	92 (+)
7	1f	(<i>R,R,R</i>)- K	-15	1:0	88%	3f	97 (+)
8	1h	(<i>R,R,R</i>)- K	-15	1:0	90%	3h	91 (+)
9 ^f	1a	(<i>R,R,R</i>)- K	-15	1:0	87%	3a	92 (+)
10 ^f	1d	(<i>R,R,R</i>)- K	-15	1:0	92%	3d	92 (+)

^a L*-AuCl [(*S,S,S*)-**I** or (*R,R,R*)-**K**] (10 mol %) and AgSbF₆ (10 mol %) in CH₂Cl₂ (0.15 M) for 1–3 h, unless otherwise noted. ^b Determined by ¹H NMR in the crude mixtures. ^c Isolated yields of pure **3**. ^d Enantiomeric excess (*ee*) determined by HPLC (Chiralcel IA).¹⁴ ^e Optical rotation sign under parentheses.¹⁴ ^f Reaction carried out with 2 mol % of (*R,R,R*)-**K** and AgSbF₆.

varied from 91% (entries 5 and 8) to a maximum value of 97%, observed for the cycloaddition of allenediene **1f** (entry 7).²⁵ Particularly relevant are the results with allenediene **1h**, cycloaddition which provides an enantioselective entry to relevant *trans*-fused 6,6-bicyclic systems. Treatment of this allenediene with catalyst (*S,S,S*)-**I**/AgSbF₆ (10 mol %) afforded the corresponding adduct (**3h**) in a moderate 52% ee, whereas (*R,R,R*)-**K**/AgSbF₆ provided **3h** in 90% yield and 91% ee (entries 4 and 8). No less significant, the catalyst loading could be significantly reduced without affecting the selectivity of the reaction. Thus, with only 2 mol % of catalyst, the cycloaddition of **1a** or **1d** provided, after 3 h at -15 °C, the desired cycloadducts in excellent yields and 92% ee (entry 9 and 10). To the best of our knowledge, the above cycloadditions represent the first examples of an efficient asymmetric process catalyzed by a mononuclear phosphorus-based carbophilic Au complex. Furthermore, this methodology constitutes one of the very few transition metal catalyzed enantioselective [4C+2C] cycloadditions of nonactivated substrates and the first of this type leading to 6,6-*trans*-fused bicyclic systems.^{26,27}

Finally, the absolute configuration of cycloadduct **3d**, prepared with (*S,S,S*)-**I**/AgSbF₆ (entry 2, 76% ee), was unambiguously determined to be (3*aR*,7*aS*) by X-ray crystallographic analysis, after recrystallization from a mixture of Et₂O/hexanes (Figure 3).²⁸

2.3. Mechanistic Experimental Studies. Key mechanistic information can be deduced from the observation that the

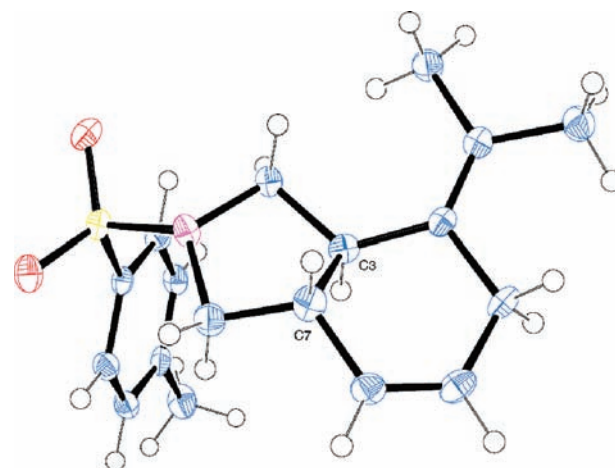


Figure 3. X-ray crystallographic structure of (3*aR*,7*aS*)-**3d**, obtained as major enantiomer in the cycloaddition of **1d** with (*S,S,S*)-**I**/AgSbF₆ (Table 4, entry 2). Flack parameter = 0.00(8).

enantiomeric excess of the major [4C+2C] cycloadduct **3a** was virtually identical (± 1 –2%) to that of the minor [4C+3C] products **2a** regardless of the phosphoramidite gold catalyst (Table 5, entries 1–11) and temperature (entries 7–9) employed. Moreover, entirely different gold-complexes, such as DTBM-Segphos(AuCl)₂ also provided the same ee values for both [4C+3C] and [4C+2C] adducts (entry 12). These results highly suggest that both cycloadditions share the same enantiodetermining step, with the resulting common intermediate evolving to either the six or the seven-membered carbocycle.

The aforementioned result could be a priori compatible with an hypothetical stepwise mechanism involving a common carbocationic intermediate such as **II** (Scheme 1). Indeed, vinyl metal species related to **II** have been previously postulated as intermediates in gold and platinum catalyzed [2+2] and [3+2] cycloadditions of allenenes.^{15,29} After the initial enantio- and diastereoselective cyclization to give **II**, an intramolecular attack from the α , or β carbon of the vinyl-gold species to the less substituted position of the generated allyl cation (6-*endo* vs 7-*endo* cyclization of **II**), would respectively lead to the formation of the [4C+2C] or [4C+3C] cycloadduct. Alternatively, a *cis-trans* isomerization of **II**, followed by a 4-*exo* cyclization on its *cis*-fused isomer (*cis*-**II**) would account for the formation of a [2C+2C] adduct.^{15a}

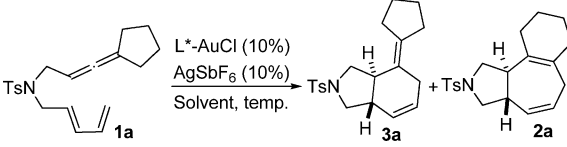
(27) Only very recently, chiral phosphoramidites have been shown effective in other transition metal catalyzed asymmetric cycloadditions with Rh, Pd or Co catalysts. For representative cases with Pd, see: (a) Shintani, R.; Park, S.; Shirozu, F.; Murakami, M.; Hayashi, T. *J. Am. Chem. Soc.* **2008**, *130*, 16174–16175. (b) Shintani, R.; Park, S.; Duan, W. L.; Hayashi, T. *Angew. Chem., Int. Ed.* **2007**, *46*, 5901–5903. (c) Shintani, R.; Murakami, M.; Hayashi, T. *J. Am. Chem. Soc.* **2007**, *129*, 12356–12357. (d) Trost, B. M.; McDougall, P. J.; Hartmann, O.; Wathen, P. T. *J. Am. Chem. Soc.* **2008**, *130*, 14960–14961. (e) Trost, B. M.; Cramer, N.; Silverman, S. M. *J. Am. Chem. Soc.* **2007**, *129*, 12398–12399. (f) Trost, B. M.; Stambuli, J. P.; Silverman, S. M.; Schworer, U. *J. Am. Chem. Soc.* **2006**, *128*, 13328–13329. For Rh, see: (g) Yu, R. T.; Lee, E. E.; Malik, G.; Rovis, T. *Angew. Chem. Int. Chem.* **2009**, *48*, 2379–2382, and references therein. For Co, see: (h) Toselli, N.; Martin, D.; Achard, M.; Tenaglia, A.; Burgi, T.; Buono, G. *Adv. Synth. Catal.* **2008**, *350*, 280–286.

(28) Comparison of optical rotations and chiral HPLC analysis allow to propose the same absolute configuration for the remaining [4C+2C] adducts obtained with (*S,S,S*)-**I**. Catalyst (*R,R,R*)-**K** provided, in every case, opposite absolute configuration than (*S,S,S*)-**I**.

(29) For a Pt-catalyzed [3C+2C] cycloaddition of allenenes: (a) Zhang, G.; Catalano, V. J.; Zhang, L. *J. Am. Chem. Soc.* **2007**, *129*, 11358–11359. (b) For two examples on Au-catalyzed [3C+2C] cycloadditions, see also ref 11.

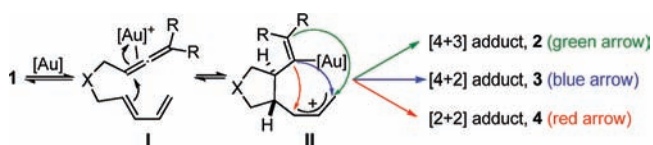
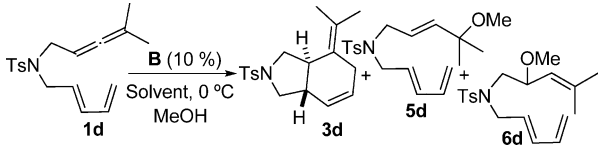
(25) Decreasing the reaction temperature to -30 °C did not bring any significant improvement on the enantioselectivity of cycloadditions with substrates **1d**, **1f**, or **1h**, neither with catalyst (*S,S,S*)-**I** or (*R,R,R*)-**K**.

(26) Previously reported examples deal with alkyne-tethered 1,3-dienes. For instance, see: (a) Shintani, R.; Sannohe, Y.; Tsuji, T.; Hayashi, T. *Angew. Chem., Int. Ed.* **2007**, *46*, 7277–7280. (b) Aikawa, K.; Akutagawa, S.; Mikami, K. *J. Am. Chem. Soc.* **2006**, *128*, 12648–12649, and references therein. (c) Gilbertson, S. T.; Hoge, G. S.; Genov, D. G. *J. Org. Chem.* **1998**, *63*, 10077–10080, and references therein.

Table 5. Comparison of the enantioselectivities of **2a** and **3a**, isolated from the reaction of **1a** using different Au catalysts.^a


entry	L*AuCl	temp. (°C)	3a:2a ^b	3a, er ^c	2a, er ^c
1	(S)-E	23	6:1	51:49	50.5:49.5
2	(S,S)-F	23	3:1	52:48	52:48
3	(S,S,S)-G	23	4.5:1	60:40	59:41
4	(R,S,S)-G	23	3:1	52:48	53:47
5	(S,S)-H	23	4:1	61:39	61:39
6	(S,R,R)-I	23	4:1	57:43	56:44
7	(S,S,S)-I	23	7:1	76:24	76:24
8	(S,S,S)-I	-15	8:1	87:13	87:13
9	(S,S,S)-I	-30	14:1	90:10	90:10
10	(R,R,R)-J	-15	8:1	90:10	91:9
11	(R,R,R)-K	-15	16:1	95.5:4.5	96:4
12 ^d	(R)-DTBM-Segphos (AuCl) ₂	23	1:1.7	54:46	54:46

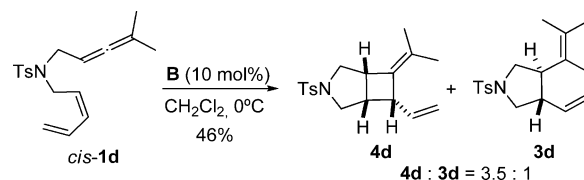
^a Conditions: **1a** (1 equiv), L*-AuCl (10 mol %) and AgSbF₆ (10 mol %) in CH₂Cl₂ (0.15 M) for 1–3 h unless otherwise noted. Conversions >99%. ^b Determined by ¹H NMR in the crude mixtures. ^c er = enantiomeric ratio (HPLC).¹⁴ ^d (R)-DTBM-Segphos (AuCl)₂ (5 mol %) and AgSbF₆ (10 mol %) was used.

Scheme 1. Hypothetical Stepwise Mechanism Involving Carbocationic Intermediate **II****Table 6.** Gold-Catalyzed Cycloadditions of **1c** in the Presence of MeOH^a


entry	solvent	MeOH	3d:5d:6d ^b
1	CH ₂ Cl ₂	3 equiv	100:0:0
2	MeNO ₂	3 equiv	85:15:0
3	MeOH	solvent	0:85:15

^a Conditions: **1d** (1 equiv, 0.15 M), **B** (10 mol %) and AgSbF₆ (10 mol %) for 1–3 h. Conversions >99%. ^b Ratios determined by ¹H NMR in the crude mixtures.

To corroborate or discard this hypothesis, we carried out several experiments in the presence of different amounts of MeOH, aiming at intercepting the allyl cation present in species **II**. However, reactions of allenediene **1d** in CH₂Cl₂ in presence of complex **B** and 3 equiv of MeOH as trapping agent, provided only the [4C+2C] cycloadduct **3d** (Table 6, entry 1). Using a more polar solvent such as MeNO₂, the reaction provided a 8.5:1.5 mixture of the [4C+2C] adducts **3d** and the acyclic compound **5d** (entry 2). This new product (**5d**) is the result of a hydroalkoxylation reaction of the allene, a type of process that has recently been shown to be efficiently promoted by related gold(I) catalysts.³⁰ Increasing the amount of MeOH did not afford any relevant product that could validate the cationic annulation pathway depicted in Scheme 1. Indeed, when MeOH was employed as solvent, the reaction led to the sole formation

Scheme 2. Gold-Catalyzed Cycloaddition Reactions of *cis*-**1d**

of the acyclic hydroalkoxylated products **5d** and its regioisomer **6d** (ratio **5d:6d** = 85:15, entry 3), while no traces of trapping products derive from **II** could be detected. Similar results were obtained from allenediene **1a**.³¹

According to the hypothesis of Scheme 1, it might be expected that an isomer of **1** bearing an internal *cis* alkene (*cis*-**1**) would lead to similar results to those obtained from the *trans* isomer **1**. However, treatment of *cis*-**1d** with catalyst **B** afforded, after 8 h at rt, a 3.5:1 mixture of the [2C+2C] and [4C+2C] adducts **4d** and **3d**, in 46% yield (Scheme 2). The acute differences in the outcomes of cycloadditions of **1d** (*trans*) and *cis*-**1d** seem to rule out the possibility that [4C+2C] and [4C+3C] cycloadditions of **1d** (*trans*), promoted by catalyst **B**, occur via a cationic cascade involving the intermediate formation of **II**.³² Moreover, *cis*-**1d** remained unchanged after several hours of treatment with PtCl₂ (110 °C) or catalyst **A** (*rt*), a result that sharply contrasts with that obtained from *trans*-**1d**, which provides the [4C+3C] cycloaddition using PtCl₂ (10 mol %), and a mixture of [4C+3C] and [4C+2C] adducts upon reaction with catalyst **A** [(IPr)AuCl/AgSbF₆, 10 mol %].¹⁴ This lack of reactivity of the *cis* precursor with these two catalysts further suggests that they do not promote the cationic cascade depicted in Scheme 1, and that the [4C+2C] adducts might be formed through an alternative mechanism.

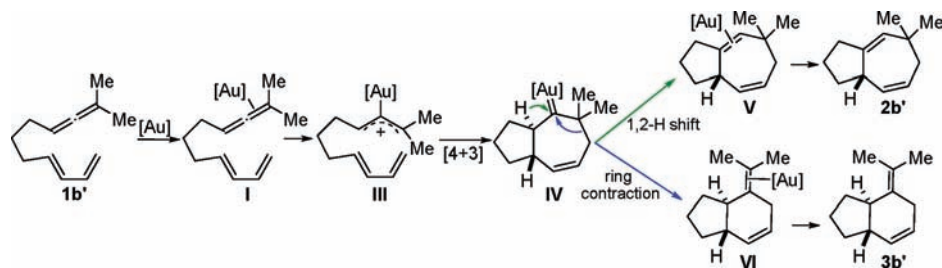
2.4. DFT Studies. Several hypothetical reaction pathways for the formation of the [4C+2C] adducts were evaluated by means of DFT calculations on the model dimethylallenediene **1b'** (Scheme 3), using [(MeO)₃PAu]⁺ as catalyst system. The validity of [(MeO)₃PAu]⁺ as model catalyst for the theoretical study of the [4C+2C] process was confirmed by experimentally running the cycloaddition reaction of **1a** in the presence of (EtO)₃PAuCl/AgSbF₆, instead of the phosphite or phosphoramidite complexes previously shown. The reaction took place with comparable rates and provided a mixture of **3a** and **2a** in a 5:1 ratio and a 95% combined yield. Analogously, the cycloaddition of **1c** with this catalyst provided a 10 to 1 mixture of **3c** and **2c** in 82% combined yield.

The cationic stepwise pathway represented in Scheme 1, involving the formation of cationic species **II**, was initially analyzed. However, in spite of an intensive exploration of the potential energy surface, not such or related species could be located.³³ This exploration also revealed that the initial activation of the allene by the phosphite gold catalyst triggers a concerted [4C+3C] cycloaddition with the diene, process which occurs

(30) Zhang, Z.; Widenhofer, R. A. *Org. Lett.* **2008**, *10*, 2079–2081. For intramolecular versions, see: (b) Zhang, Z.; Liu, C.; Kinder, R. E.; Han, X.; Qian, H.; Widenhofer, R. A. *J. Am. Chem. Soc.* **2006**, *128*, 9066–9073, and references therein.

(31) Reaction of allenediene **1a** with catalyst **B** (10 mol %), in the presence of 3 equiv of MeOH, provided the same ratio of [4C+3C] and [4C+2C] products as obtained in the absence of MeOH (**2a:3a** ratio = 1:10).

(32) In consonance with this proposal, Toste et. al. reported that a related allenediene selectively mono deuterated at the terminal position of the diene provided a stereoselective [4C+2C] cycloaddition, making very unlikely a cationic pathway involving species such as **II** (see ref 11).

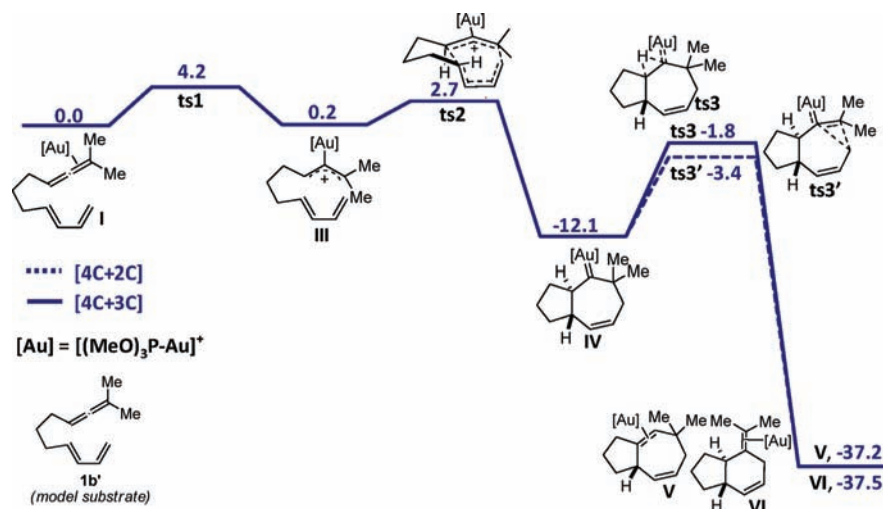
Scheme 3. Mechanistic Proposal for a [4C+2C] Process Resulting from an Initial [4C+3C] Cycloaddition and a Subsequent Ring Contraction (Blue Arrow)

with an extremely low energy barrier. This fact together with the experimental information indicating that both [4C+2C] and [4C+3C] cycloadditions are stereospecific processes sharing a common stereo and enantio-determining step, led as to consider a mechanistic scenario in which the [4C+2C] cycloadduct could be eventually generated after an initial concerted [4C+3C] cycloaddition of the allenediene leading to Au-carbene **IV** (Scheme 3). Indeed, the DFT calculations revealed that the [4C+2C] adduct **3b'** might result from an internal 1,2-alkyl migration (ring contraction) on the cycloheptenyl carbene intermediate **IV**, itself arising from the concerted [4C+3C] cycloaddition of **III** (Scheme 3).

The reaction mechanism for the Au-catalyzed [4C+3C] cycloaddition of allenedienes leading to products of type **2** through the intermediacy of cycloheptenyl carbene **IV** was recently described employing AuCl, AuCl₃ and [(NHC)Au]⁺ as model gold catalysts.^{10b} A DFT analysis of the mechanism using [(MeO)₃PAu]⁺ as catalyst gives similar reaction pathways to those previously found for the former Au catalysts. The set of steps describing the mechanism involves initial catalyst coordination to the allene (**I**), generation of the metal-allyl intermediate (**III**), and [4C+3C] concerted cycloaddition providing the cycloheptene structure (**IV**). At this point, this intermediate might evolve by means of an standard 1,2-H-shift giving rise to the final [4C+3C] cycloaddition product **2b'**. However, DFT calculations also confirm the viability of a different scenario in which the same intermediate (**IV**) can evolve by means of an internal 1,2-alkyl migration (ring contraction), giving rise to the [4C+2C] cycloaddition product **3b'** (Scheme 3, Figure 4). Such mechanistic divergence from intermediate **IV** is in full agreement with the formation of both

types of adducts in the cycloaddition of allenedienes **1b** and **1c** catalyzed by complex **B** (Table 2, entries 1–3) or (EtO)₃PAuCl/AgSbF₆. Furthermore, it is in total agreement with the asymmetric results with phosphoramidite gold catalysts, since both [4C+3C] and [4C+2C] pathways are sharing the same stereo and enantio-determining step, a concerted *exo*-like [4C(4π)+3C(2π)] cycloaddition between the diene and the Au-allyl cation (from **III** to **IV**). The chemoselective differentiation takes place in a posterior step (from **IV** to **V**/**VI**).³⁴ Finally, it is also consistent with the requirement of a *trans*-diene to achieve an efficient [4C+2C] cycloaddition, since it is mandatory for the initial [4C+3C] concerted cycloaddition leading to **IV**.³⁵

The overall energy profiles for the mechanism, including the divergence from intermediate **IV**, are shown in Figure 4. The two initial steps are common for both pathways. They start with the initial coordination of the allene to the metal center, **I** (selected as energy reference). This species evolves to the formation of a Au-allyl cation intermediate, **III**, through an energy barrier of 4.2 kcal/mol (**ts1**). The energy of **III** is 0.2 kcal/mol compared to **I**. This precursor easily gives rise to a 7-membered ring intermediate **IV** through a concerted cycloaddition (**ts2**) with a small relative energy barrier of 2.5 kcal/mol. The structure of this transition step is depicted in Figure 5. Interestingly, the formation of the two σ -bonds in this step is much more asynchronous than with any of the other gold catalyst previously investigated in [4C+3C] allenediene cycloadditions.^{10b} Cycloheptene-gold species **IV** is the most stable intermediate within the reaction profile with a relative energy of -12.1 kcal/mol. **IV** can evolve in two ways: by a 1,2-hydrogen shift to **V** (**ts3**) or by a 1,2-alkyl migration (ring contraction, **ts3'**) to **VI**. Each of the products is obtained with

**Figure 4.** DFT profile for the cycloaddition of a model substrate **1b'** with [(MeO)₃PAu]⁺.

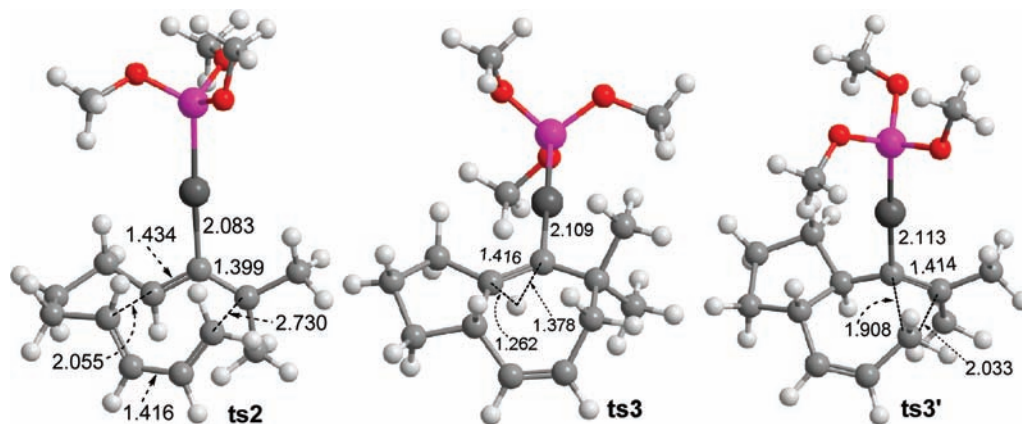


Figure 5. DFT calculated structures for concerted cycloaddition (**ts2**), the 1,2-H shift (**ts3**) and ring contraction (**ts3'**) transition states, leading to the corresponding [4C+3C] and [4C+2C] cycloadducts **V** and **VI**.

the new formed C–C double bond coordinated to the Au metal center. The energy barriers for these two competitive pathways are 10.3 and 8.7 kcal/mol, respectively.³⁶ These data are reasonably consistent with the experimental results which indicate that the energy barrier associated to each of the routes must not be too different since both products are observed, although the formation of the [4C+2C] adduct is slightly favored. The transition states corresponding to the 1,2-H shift (**ts3**) and 1,2-ring contraction (**ts3'**), respectively leading to the [4C+3C] and [4C+2C] cycloadducts **V** and **VI**, are depicted in Figure 5.

We also analyzed these pathways with other Au complexes such as [(PH₃)Au]⁺, as a model for Ph₃PAuCl/AgSbF₆, [(NHC)Au]⁺, as a model for catalyst **A**,^{10b} and AuCl. As can be deduced from the energetic data of Table 7 the difference in energy barriers between the 1,2-H migration and the 1,2-ring contraction is not high, confirming that both pathways are competitive. It can be observed that the more electron acceptor is the ligand at gold the more favored is the internal 1,2-alkyl migration that leads to the [4C+2C] adduct, a result in

Table 7. Calculated Energy Barriers for Competitive Migration Steps with Substrate **1b'** (kcal/mol)

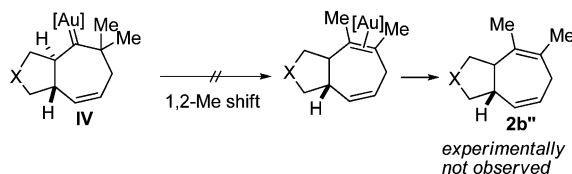
entry	catalyst	1,2-H migration barrier ($E_{ts3} - E_{IV}$)	1,2-alkyl migration barrier ($E_{ts3'} - E_{IV}$)	ΔE
1	[(MeO) ₃ PAu] ⁺	10.3	8.7	-1.6
2	[(PH ₃)Au] ⁺	8.1	8.5	0.4
3	AuCl	14.6	17.7	3.1
4	[(NHC)Au] ⁺	8.7	10.8	2.1

agreement with experimental observations. Thus, the highest energy barrier difference ($E_{ts3'} - E_{ts3}$) in favor of the [4C+2C] adduct is found for [(MeO)₃PAu]⁺ catalyst. [H₃PAu]⁺ afforded similar barriers for both processes (0.4 kcal/mol difference), whereas the highest difference in favor of the [4C+3C] cycloadduct corresponds to AuCl and [(NHC)Au]⁺, catalysts that have been successful used for this type of cycloadditions.^{10b} The calculations with AuCl gave rise to a energy barrier difference ($E_{ts3} - E_{ts3'}$) slightly superior to 3 kcal/mol (entry 3), whereas for the cationic catalyst [(NHC)Au]⁺ the difference is of 2.1 kcal/mol, again favoring the formation of the [4C+3C] adduct (entry 4). The higher reactivity experimentally observed with [(NHC)Au]⁺, as compared to AuCl, is reflected in the lower energy barrier associated to the transformation of **IV** into **V** (8.7 vs 14.6 kcal/mol, entries 3 and 4), a step that has been postulated as rate determining for the [4C+3C] cycloadditions.

The precise reasons why an electron acceptor ligand at gold might favor the 1,2-ring contraction, whereas an electron donating one preferentially promotes the 1,2-H shift, are not easy to identify. Steric reasons depending on the ligand structure might not be critical, since different gold catalysts with more or less sterically demanding acceptor ligands provided similar results (i.e., (EtO)₃PAuCl/AgSbF₆ vs catalyst **B**). It is plausible, however, that the electronic factors such as the interaction between the new double bond being generated at **ts3** or **ts3'**

(33) A cationic structure keeping frozen the C–C distance of the new formed C–C bond (forming the 5-membered ring) resembling the structure of **II** was optimized. Nonetheless, when performing a full geometry optimization starting from this *forced* structure, it always evolved to initial reactants breaking the C–C bond, therefore suggesting that this is not a stable species.

(34) An alternative 1,2-methyl shift on intermediate **IV** might also be proposed and would lead to a [4C+3C] cycloadduct of type **2b''** (see equation below). However, this cycloadduct was never observed in the cycloaddition of **1b**. This type of 1,2-alkyl migration was only observed when the allene has a cyclic substituent at the distal position, such as in **1a**. Apparently, the release of strain associated with the 1,2-alkyl shift allows to overcome the preference of a 1,2-H shift. For reviews on migratory aptitudes of different substituents on metal carbenes, see: (a) Crone, B.; Kirsch, S. F. *Chem.–Eur. J.* **2008**, *14*, 3514–3522. (b) Nickon, A. *Acc. Chem. Res.* **1993**, *26*, 84–89. (c) Liu, M. T. H. *Acc. Chem. Res.* **1994**, *27*, 287–294]



(35) The minor formation of the [4C+2C] adduct **3d** from *cis*-**1d** (vide supra), might be explained by a partial *Z/E*-isomerization (see ref 15a). Alternatively, cationic stepwise mechanisms operating from *cis*-**1d** cannot be fully discarded. For instance, see: Gassman, P. G.; Singleton, D. A. *J. Org. Chem.* **1984**, *106*, 6085–6086.

(36) The 1,2-H shift leading to **V** is actually a two step process: the first one with a 8.6 kcal/mol activation barrier corresponds to an axial-to-equatorial conformational change on the seven-membered ring to obtain the appropriate parallel disposition of the orbitals implicated in the subsequent 1,2-H shift; this intermediate, **IV'**, lies 8.1 kcal/mol over **IV**. The second step is the 1,2-H shift properly speaking with an activation barrier of 2.2 kcal/mol. The energy barrier for the transformation of **IV'** to **IV** is so small (0.5 kcal/mol), that in practice, the evolution from intermediate **IV** to the product **V** can be considered taking place in a single step. Thus, for clarity reasons, we depicted this process in Figure 4 as a single step with the overall barrier of 10.3 kcal/mol. For a complete description of this process, see the Supporting Information.

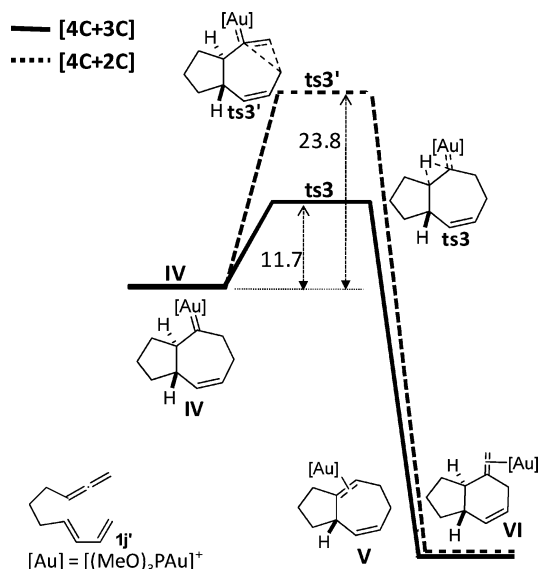


Figure 6. Cycloaddition of model substrate $1j'$: energy profile involving the 1,2-alkyl migration ($ts3'$) and 1,2-H migration ($ts3$).

with the highly electrophilic gold atom could play a key role. Indeed, the *exocyclic* double bond which is being generated in the ring contraction process ($ts3'$) might easily optimize its orientation in such a way that donation from the occupied π -orbitals to the electrophilic gold metal center is maximized, and therefore $ts3$ could be favored when an electron acceptor ligand is placed at gold (i.e., phosphites or phosphoramidites). Conversely, the *endocyclic* double bond formed at $ts3$, could have more conformational restrictions to fully optimize such interaction and, accordingly, a transition state $ts3$, leading to **V**, might not be particularly favored with such highly electrophilic gold complexes.

Albeit [4C+3C] cycloaddition products have been observed for [(NHC)Au]⁺-catalyzed reactions of substrates in which the allene is monosubstituted at the C-terminus position,^{10b} we never observed [4C+2C] adducts from these substrates using [(RO)₃PAu]⁺. Therefore, we carried out DFT calculations to quantify the eventual dependence of the ring contraction step on the presence of substituents at the allene C-terminus. The proposed mechanisms for the formation of [4C+2C] and [4C+3C] adducts were theoretically evaluated with [(MeO)₃PAu]⁺ for the model substrate $1j'$, which includes hydrogen atoms instead of methyl groups at the distal position of the allene (Figure 6). The mechanisms for the formation of the two different products are qualitatively similar to those previously commented and share the two initial steps. Once the 7-membered ring intermediate **IV** is formed, the relative energy barrier for the 1,2-H-shift (formation of [4C+3C] product) is 11.7 kcal/mol. For the case of the 1,2-alkyl migration (formation of [4C+2C] product), however, the relative energy barrier is 23.8 kcal/mol (Figure 6). According to these values, the formation of [4C+2C] cycloadduct seems to be strongly dependent on the presence of a quaternary center at the adjacent position of the Au-carbene center (see the Supporting Information for more details).

In summary, the calculations have provided interesting information into the plausible mechanistic bases of the [4C+3C] and [4C+2C] divergence. The nature of the ligand guides the formation of the final product: the more electron withdrawing

is the ligand the more favored is the formation of the [4C+2C] product. However, other mechanisms cannot yet be fully discarded.

3. Conclusions and Outlook

In summary, we report a new Au-catalyzed [4C+2C] cycloaddition of allenediene, along with a highly asymmetric variant promoted by novel phosphoramidite-gold catalysts. Indeed, these reactions represent the first processes in which a gold complex derived from a phosphoramidite or any other type of monodentate ligand acts as an efficient carbophilic chiral catalyst. We have also reported mechanistic studies suggesting that the divergence between [4C+2C] and [4C+3C] paths might arise from relative 1,2-migration tendencies in a common cycloheptenyl Au-carbene intermediate. Current efforts are focused to further mechanistic studies, synthetic applications and the use of these new phosphoramidite complexes to other Au-catalyzed transformations.

4. Experimental Section

Computational Details. Calculations were performed with the Gaussian03 program package³⁷ at density functional theory (DFT) level by means of the hybrid B3LYP functional.³⁸ For geometry optimization, the main group elements (C, Cl, O, N, P, H) were described using the 6-31G(d) basis set (labeled as basis set I). The Au metal center was described by the LANL2DZ effective core potential³⁹ and its associated basis set for the outermost electrons. An extra series of f-polarization functions were also added for Au atom (Au: exp. = 1.050).⁴⁰ Moreover, additional single point calculations using the 6-311++G(d,p) basis set for all the main group elements were also performed (basis set II), including solvent effects by means of the CPCM method (CH₂Cl₂; ϵ = 8.93) (see Supporting Information).

The geometries of the reactants, intermediates, transition states, and products were fully optimized without any symmetry restriction. Frequency calculations were performed on all optimized structures (at the optimization level) to characterize the stationary points as minima (non imaginary frequencies) or transition states (one imaginary frequency).

General Procedure for the [4C+2C] Cycloaddition of Allenediene **1 (Exemplified for **1a**).** A solution of compound **1a** (100 mg, 0.291 mmol) in CH₂Cl₂ (0.8 mL) was added to a suspension of (ArO)₃PAuCl (25.6 mg, 0.029 mmol) and AgSbF₆ (10.0 mg, 0.029 mmol) in CH₂Cl₂ (1.2 mL) in a dried Schlenk tube under argon, at 0 °C. The mixture was stirred at that temperature for 3 h and filtered through a short pad of florisil eluting with Et₂O. The filtrate was concentrated and purified by flash chromatography (10–15% Et₂O/hexanes) to afford 72 mg of a 1:10 mixture of cycloadducts **2a** and **3a** (72%, **2a**:**3a** = 1:10).

(3aR*,7aS*)-4-Cyclopentylidene-2-tosyl-2,3,3a,4,5,7a-hexahydro-1H-isoindole (3a). ¹H NMR (500 MHz, CDCl₃): δ (ppm) 7.73 (d, J = 8.3 Hz, 2H), 7.31 (d, J = 8.0 Hz, 2H), 5.71 (s, 2H), 3.87 (dd, J = 9.4 and 5.8 Hz, 1H), 3.63 (dd, J = 9.1 and 7.1 Hz, 1H), 3.37 (t, J = 10.1 Hz, 1H), 2.86 (dd, J = 10.9 and 9.2 Hz, 1H), 2.70 (d, J = 21.2 Hz, 1H), 2.66 (d, J = 21.9 Hz, 1H), 2.42 (s,

(37) Frisch, M. J. et al. *Gaussian 03, Revision C.02*; Gaussian, Inc.: Wallingford CT, 2004. (See Supporting Information, ref 21.)

(38) (a) Lee, C.; Parr, R. G.; Yang, W. *Phys. Rev.* **1988**, *37*, B785. (b) Becke, A. D. *J. Chem. Phys.* **1993**, *98*, 5648–5652. (c) Stephens, P. J.; Devlin, F. J.; Chabalowski, C. F.; Frisch, M. J. *J. Phys. Chem.* **1994**, *98*, 11623–11627.

(39) (a) Hay, P. J.; Wadt, W. R. *J. Phys. Chem.* **1985**, *82*, 299. (b) Wadt, W. R.; Hay, P. J. *J. Chem. Phys.* **1985**, *82*, 284–298.

(40) Höllwarth, A.; Böhme, M.; Dapprich, S.; Ehlers, A. W.; Gobbi, A.; Jonas, V.; Köhler, K. F.; Stegman, R.; Veldkamp, A.; Frenking, G. *Chem. Phys. Lett.* **1993**, *208*, 237–240.

3H), 2.30–2.14 (m, 4H), 1.76–1.50 (m, 4H); ^{13}C NMR (125.8 MHz, CDCl_3): δ (ppm) 143.2 (C), 136.1 (C), 134.7 (C), 129.7 (CH), 128.8 (CH), 127.2 (CH), 125.3 (CH), 122.2 (C), 51.3 (CH_2), 50.8 (CH_2), 47.1 (CH), 42.8 (CH), 32.0 (CH_2), 31.6 (CH_2), 30.9 (CH_2), 27.4 (CH_2), 25.8 (CH_2), 21.5 (CH_3). LRMS (m/z , I): 343 ($[\text{M}^+$], 9), 188 (97), 154 (29), 91 (100). HRMS calculated for $\text{C}_{20}\text{H}_{25}\text{NO}_2\text{S}$ 316.16060, found 316.16061. Further confirmation of the structure of **3a** was obtained by X-ray crystallography. The remaining cycloadducts of Table 2 were prepared using this procedure and their spectroscopic data can be found in the Supporting Information.

General Procedure for the [4C+2C] Cycloaddition of Alkenedienes **1 with Phosphoramidite-Based Gold Catalysts (Exemplified for **1a** with (*R,R,R*)-**K**).** A solution of compound **1a** (100 mg, 0.291 mmol) in CH_2Cl_2 (0.8 mL) was added to a suspension of [(*R,R,R*)-**K**] (6.55 mg, 5.82 μmol , 2 mol %) and AgSbF_6 (2.0 mg, 5.82 μmol , 2 mol %) in CH_2Cl_2 (1.2 mL) in a dried Schlenk tube, under argon, at -15°C . The mixture was stirred at that temperature for 3 h (the progress of the reaction was easily monitored by *tlc*) and filtered through a short pad of florisil eluting with Et_2O . The filtrate was concentrated and purified by flash chromatography (10–15% Et_2O /hexanes) to afford 87 mg of

cycloadduct **3a** (87% yield). HPLC analysis on Chiralcel IA (0.5 mL/min, hexane: *i*-PrOH = 99: 1) showed a 92% enantiomeric excess (retention times: 55.1 min, major enantiomer; 61.7 min, minor enantiomer).

Acknowledgment. This research was supported by the Spanish MICINN [SAF2007-61015, CTQ2008-06866-CO2-02, Consolider-Ingenio 2010 (CSD2007-00006)], Xunta de Galicia (GRC2006/132 and PGIDIT06PXIB209126PR), CSIC and Comunidad de Madrid (CCG08-CSIC/PPQ3548). B.T. and S.M. thank the Spanish MICINN for each FPU fellowship. I.A. thanks the Xunta de Galicia for a fellowship. We thank Johnson-Matthey for a gift of metals and Takasago for a gift of (*R*)-DTBM-Segphos.

Supporting Information Available: Full experimental procedures, spectroscopy data, crystallographic information files and energies and Cartesian coordinates of optimized geometries. This material is available free of charge via the Internet at <http://pubs.acs.org>.

JA905415R